

ELECTRIC FIELD GRADIENTS IN THE IONIC CRYSTALS NaNO_2 , NaBF_4 , NaNO_3 , AND $\text{Ba}(\text{NO}_3)_2$

H. M. MAURER, P. C. SCHMIDT and ALARICH WEISS

Institut für Physikalische Chemie, Physikalische Chemie III, Technische Hochschule, Petersenstr. 20, D-6100 Darmstadt (W. Germany)

(Received 18 March 1977)

ABSTRACT

The electric field gradients (EFG) at the sites of the cations and the "central" atoms of the anions in the ionic crystals NaNO_2 , NaBF_4 , NaNO_3 , and $\text{Ba}(\text{NO}_3)_2$ are calculated by a method based on a combination of the semi-empirical INDO method for the charge distribution and the intramolecular EFG with a lattice summation in the framework of the extended multipole model. At some lattice sites the contribution of the induced dipole and quadrupole moments to the EFG is comparable with the contribution of the point charges. The charge distribution within the molecular ions is found by adjusting either the calculated asymmetry parameter η or the z -component of the EFG to the experimental value deduced from nuclear quadrupole coupling constants. These charge distributions are in good agreement with those gained from INDO calculations. The calculated and experimental quadrupole coupling constants of nuclei in anions and cations are compared.

INTRODUCTION

From nuclear quadrupole resonance (NQR) and other experiments, such as Mössbauer studies, microwave spectroscopy, etc., the nuclear quadrupole coupling constant (QCC) can be determined. The QCC is described by e^2qQ/h , where e is the unit charge, Q the nuclear quadrupole moment in units of an area, and h Planck's constant. With known values of Q the electric field gradient (EFG) $q = q_{\text{exp}}$ at the site of the nucleus considered can be determined from the experiment. Furthermore, $q = q_{\text{calc}}$ may be found from a theoretically determined charge distribution model of the atom, molecule, or solid considered.

Restricting the discussion here to NQR results, for the determination of q_{calc} the charge distribution $\rho(r)$ in a solid has to be found and compared with q_{exp} . It is shown here that for ionic crystals incorporating spherical atomic ions as well as molecular ions, a combination of MO-calculations with the multipole model is a useful method of obtaining $e^2q_{\text{calc}}Q/h$. By MO-calculations the charge distribution of the molecular ions (NO_2^- , NO_3^- , BF_4^-) is found, whereas the charge distribution of the whole lattice is deduced from the multipole model.

EXTENDED MULTIPOLE MODEL

The EFG at the site of the nucleus considered is composed of an internal contribution q_{int} , produced by the electrons belonging to the ion considered, and of an external contribution q_{ext} , created by all other charges within the crystal of theoretically infinite size. In the framework of the Sternheimer model the total EFG is given by

$$q = q_{\text{ext}} + q_{\text{int}} = q_{\text{ext}}(1 - \gamma_{\infty}) \quad (1)$$

where γ_{∞} is the anti-shielding factor (Sternheimer factor). The parameter $q_{\text{int}} = -\gamma_{\infty} q_{\text{ext}}$ takes into account the deformation of the atomic (ionic) electron cloud by the external EFG. In a first step, q_{ext} is calculated by using the point charge model [1], in which the assumption is made that spherically symmetric charge densities may describe the ions. Then the external EFG at the nucleus j is given by

$$V_{nm}^P(r_j) = \sum_i \left(Z_i \sum_l \frac{|r_{jil}|^2 \delta_{nlm} - 3x_{mjl}x_{njl}}{|r_{jil}|^5} \right) \quad (2)$$

where $r_{jil} = r_j - r_i - l_1 a_1 - l_2 a_2 - l_3 a_3$ and $x_n, x_m = x, y, z$. r_j is the site of the nucleus considered. r_i is the site of the nucleus i within the first unit cell (the unit cell containing r_j). a_1, a_2 , and a_3 are the basic vectors of the unit cell (see Fig. 1), l_1, l_2 and l_3 are integers. Z_i is the charge of the ion i . The point $r_{jil} = 0$ has to be omitted during the summation. If the directions x, y and z are parallel to the principal axes of the EFG, q_{ext} is equal to V_{zz}^P . By definition: $|V_{zz}| \geq |V_{yy}| \geq |V_{xx}|$; $V_{xx} + V_{yy} + V_{zz} = 0$; $(V_{xx} - V_{yy})/V_{zz} = \eta$; $0 \leq \eta \leq 1$. η is called the asymmetry parameter.

Assuming adjustable charge numbers Z_i , including non-integer values, a first empirical correction of this model results. Z_i can be varied until "best" agreement between q_{calc} and q_{exp} is found. Although such a procedure is applied in the literature, it is unsatisfactory [1-3]. Quite often the point charge model fails completely.

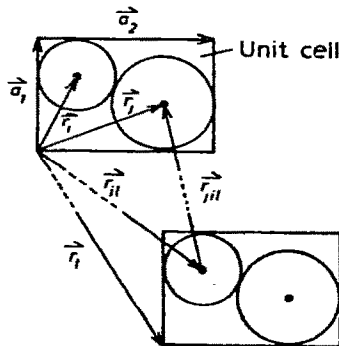


Fig. 1. Explanation of symbols used for the lattice summation. r_j is the site of the nucleus considered. r_i is the site of the nucleus i inside the first unit cell. a_1, a_2 , and a_3 are the basis vectors of the unit cell.

The point charge model can be improved by considering the polarizability of the ions in the solid. The induced dipole moment $\mathbf{p}(\mathbf{r}_k)$ and quadrupole moment $Q_{nm}(\mathbf{r}_k)$ of the ion k can be written as

$$\mathbf{p}(\mathbf{r}_k) = \alpha_k^D \mathbf{E}(\mathbf{r}_k) \quad (3)$$

$$Q_{nm}(\mathbf{r}_k) = \alpha_k^Q V_{nm}(\mathbf{r}_k) \quad (4)$$

$\mathbf{E}(\mathbf{r}_k)$ is the electric field at \mathbf{r}_k , $V_{nm}(\mathbf{r}_k)$ is the EFG at \mathbf{r}_k , and α_k^D and α_k^Q are the dipole and quadrupole polarizabilities of the ions. $\mathbf{E}(\mathbf{r}_k)$ is given by the sum of the monopole field $\mathbf{E}^P(\mathbf{r}_k)$, the dipole field $\mathbf{E}^D(\mathbf{r}_k)$, and the quadrupole field $\mathbf{E}^Q(\mathbf{r}_k)$

$$\mathbf{E}(\mathbf{r}_k) = \mathbf{E}^P(\mathbf{r}_k) + \mathbf{E}^D(\mathbf{r}_k) + \mathbf{E}^Q(\mathbf{r}_k) \quad (5)$$

Similarly the EFG is given by

$$V_{nm}(\mathbf{r}_k) = V_{nm}^P(\mathbf{r}_k) + V_{nm}^D(\mathbf{r}_k) + V_{nm}^Q(\mathbf{r}_k) \quad (6)$$

However $\mathbf{E}(\mathbf{r})$ and $V_{nm}(\mathbf{r})$ must be calculated in a self-consistent procedure to incorporate the EFG within the framework of this extended point charge model. Starting with the calculation of the field generated by the point charges

$$\mathbf{E}^P(\mathbf{r}_k) = \sum_i (Z_i \sum_l \mathbf{r}_{kil} / |\mathbf{r}_{kil}|^3) \quad (7)$$

the dipole moments have to be determined according to eqn. (3) (see Fig. 2). Then the field $\mathbf{E}^D(\mathbf{r})$, generated by the induced dipole moments, is

$$\mathbf{E}^D(\mathbf{r}_k) = \sum_{i,l} \left[\frac{3\mathbf{r}_{kil}(\mathbf{p}_i \cdot \mathbf{r}_{kil})}{|\mathbf{r}_{kil}|^5} - \frac{\mathbf{p}_i}{|\mathbf{r}_{kil}|^3} \right] \quad (8)$$

In the next step, the dipole moments generated by $\mathbf{E}^P + \mathbf{E}^D$ have to be calculated until self-consistency is reached for the dipolar field $\mathbf{E}^D(\mathbf{r})$. Then $V_{nm}^D(\mathbf{r})$ is determined. A self-consistent calculation of $V_{nm}^Q(\mathbf{r})$ is necessary. The determination of $\mathbf{E}^Q(\mathbf{r})$ follows. At this point, in a feedback step $\mathbf{E}^D(\mathbf{r})$ is recalculated (see Fig. 2).

There are two problems in calculating the values of the lattice sums:

- (a) some of the sums (e.g. the sum in eqn. 7) are not absolutely convergent, and, therefore, the result of the summation is a function of its order [4, 5];
- (b) the convergence of the sum is very slow.

Considering the conditionally convergent series, there are two possibilities for a correct summation. Either one transforms the lattice sum into two rapidly converging series over the reciprocal lattice and the real lattice according to the periodicity of the lattice, or (the method used here) one constructs partial sums and the sum of these partial sums is absolutely convergent. To reach an absolutely converging sum, a $1/r^4$ decrease of the summands is needed (r is the distance from the reference point). For example, the sum in eqn. (2) is conditionally convergent, because the EFG generated by the point charges decreases as $1/r^3$. If one adds up first over the unit cell,

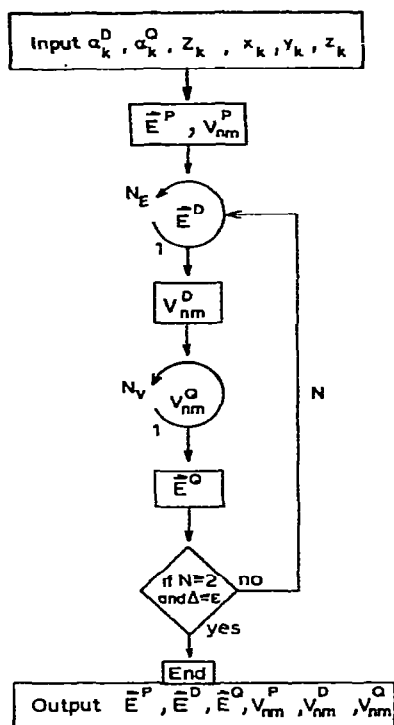


Fig. 2. Scheme of the self-consistent calculation of the electric field gradient on the basis of the multipole model. N_E , N_V , and N are the numbers of the self-consistent cycles.

that is, over the index i , the resulting sum over l_1 , l_2 , and l_3 is absolutely convergent since the partial sums over i include the same number of negative and positive charges. For large distances r the sum over the partial sums behaves like the EFG created by dipoles (or quadrupoles if the total charge and the total dipole moment of the unit cell vanish), which decreases as $1/r^4$.

A somewhat more complicated situation has to be considered for the electric field because the field generated by point charges decreases as $1/r^2$ (see eqn. 7). The summation over neutral regions has a $1/r^3$ dependence. An additional lattice can be constructed to obtain a quadrupole boundary of summation, see Fig. 3(b), which cancels the dipole moment of the boundary but does not contribute to the electric field at the point r_j considered.

To explain the method in detail, we shall restrict ourselves to the one-dimensional case. In Fig. 3(a) the real lattice is shown. The field component E_x at the point x_j will be calculated. The sum

$$\begin{aligned}
 E_x(x_j) = & Z \frac{x_1 - x_j}{(|x_1 - x_j|)^3} - Z \frac{-a_1 + x_2 - x_j}{(|-a_1 + x_2 - x_j|)^3} - Z \frac{x_2 - x_j}{(|x_2 - x_j|)^3} \\
 & + Z \frac{-a_1 + x_1 - x_j}{(|-a_1 + x_1 - x_j|)^3} + Z \frac{a_1 + x_1 - x_j}{(|a_1 + x_1 - x_j|)^3} \pm \dots
 \end{aligned} \quad (9)$$

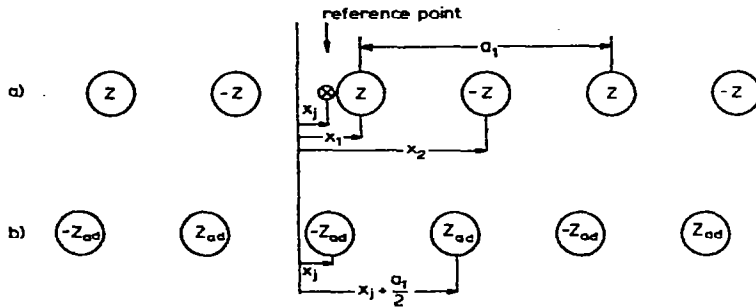


Fig. 3. (a) Linear chain model for the calculation of lattice sums involving dipole boundaries. The electric field is calculated at the point x_j . a_1 is the length of the one-dimensional unit cell, x_1 and x_2 are the positions of the charges $+Z$ and $-Z$. (b) Additional one-dimensional lattice for the compensation of the dipole moment of chain (a). The additional charges Z_{ad} do not produce an electric field at the reference point x_j .

has a monopole boundary. If one adds up first over the point charges in the unit cell, the sum has a dipole boundary

$$E_x(x_j) = \sum_{l_1=-\infty}^{+\infty} \left[Z \frac{a_1 l_1 + x_1 - x_j}{(|a_1 l_1 + x_1 - x_j|)^3} - Z \frac{a_1 l_1 + x_2 - x_j}{(|a_1 l_1 + x_2 - x_j|)^3} \right] \quad (10)$$

The partial sums discussed above are indicated by square brackets. For the quadrupole boundary the sites of the additional charges Z_{ad} are chosen in such a manner that the point x_j is a centre of symmetry for the additional lattice

$$E_{x,ad}(x_j) = Z_{ad} \frac{a_1/2}{(|a_1/2|)^3} - Z_{ad} \frac{a_1}{|a_1|^3} + \dots + Z_{ad} \frac{-a_1/2}{(|-a_1/2|)^3} - Z_{ad} \frac{-a_1}{|-a_1|^3} \dots = 0 \quad (11)$$

Z_{ad} is selected so that the dipole moment of the additional lattice is opposite to the dipole moment of the real lattice. Here simply $Z_{ad}(x_j + a_1) = -Z$ and $Z_{ad}(x_j + 0.5a_1) = +Z$. $E_x(x_j)$ is found by adding up the contributions of both the real and the additional lattice. Doing so, one finds a quadrupole boundary

$$E_x(x_j) = \sum_{l_1=-\infty}^{+\infty} \left[Z \frac{a_1 l_1 + x_1 - x_j}{(|a_1 l_1 + x_1 - x_j|)^3} - Z \frac{a_1 l_1 + x_2 - x_j}{(|a_1 l_1 + x_2 - x_j|)^3} + Z_{ad} \frac{a_1 l_1 + a_1/2}{(|a_1 l_1 + a_1/2|)^3} - Z_{ad} \frac{a_1 l_1}{(|a_1 l_1|)^3} \right] \quad (12)$$

This method can be generalized easily to the three-dimensional case [6]. The summation in the real lattice (compared with the summation in the reciprocal lattice) has the advantage that one single computer program can be developed for all crystals, independent of the symmetry, the sites, and the number of ions in the unit cell.

The second problem is the unsatisfactory convergence of the sums. Because of the restriction to a limited number of summands, an extrapolation method [7] must be applied. Here a method proposed by Coogan [8] is chosen. The sum is taken over all unit cells within the limit

$$-N \leq l_1, l_2, l_3 \leq N; N = 1, 2, 3 \dots$$

The partial sums S_N are monotonic functions of N . Plotting S_N as a function of $(2N + 1)^{-2}$, nearly straight lines are found (Fig. 4) and extrapolation is simple.

The charge distribution of the ions NO_2^- , NO_3^- , and BF_4^- were found from the semi-empirical MO-methods CNDO/2 [9], INDO, and their versions CNDO/2D and INDO/D [10, 11], respectively. With these methods the netto charges n_a and the brutto charges N_a , as defined by Mullikan [12], were calculated

$$n_a = Z'_a - \sum_{\mu}^a P_{\mu\mu} \quad (13)$$

and

$$N_a = n_a - \sum_{\mu}^a \sum_{\nu}^{b \neq a} P_{\mu\nu} \langle \varphi_{\mu} | \varphi_{\nu} \rangle \quad (14)$$

φ_{μ} and φ_{ν} are the basis functions and $P_{\mu\nu}$ is an element of the density matrix. Z'_a is the core charge of the atom a . The index μ runs over all atomic orbitals of the valence shell of it. For CNDO and INDO n_a and N_a are equal.

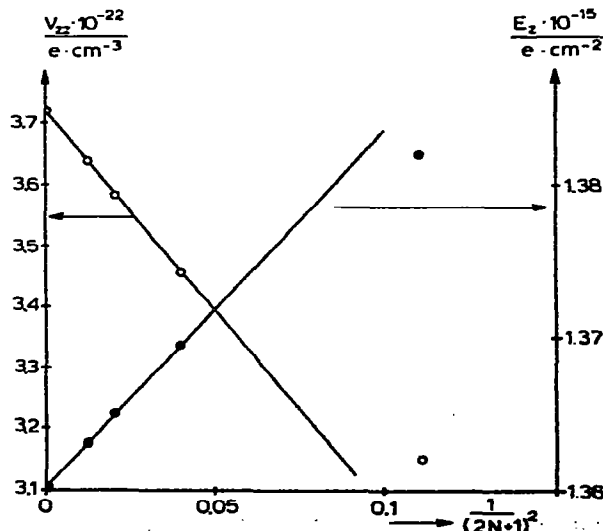


Fig. 4. Value of the electric field at the site of the oxygen and the electric field gradient at the site of the sodium in NaNO_3 for various values of the boundary parameter N . e is given in electrostatic units.

In the compounds discussed here, the charge distributions of the complex ions (eqn. 14) were used for the self-consistent EFG calculations (see eqns. 2 and 7) [13] at the site of ^{23}Na and ^{137}Ba , respectively. In determining the EFG at the site of ^{14}N and ^{11}B , i.e. at sites within the complex ions considered, two parts of the EFG are important. The first one, created by all multipoles outside the complex ion of interest, is calculated by the self-consistent procedure shown above. The second, the "internal" EFG of the molecular ion, is due to the charge distribution of the molecule ion itself and is given by

$$V_{nm}^{\text{mol}}(\mathbf{r}_b) = \sum_{a \neq b} Z_a \frac{3x_{na}x_{ma} - \delta_{nm}r_a^2}{r_a^5} - 2e \sum_i \left\langle \Psi_i \left| \frac{3x_n x_m - r^2 \delta_{nm}}{r^5} \right| \Psi_i \right\rangle \quad (15)$$

Here the first summand is due to the nuclei with the charges Z_a located at the points $\mathbf{r}_a = (x_{1a}, x_{2a}, x_{3a})$ and the second term gives the contribution of the electrons. Within the framework of the semi-empirical calculations used here, this is given by

$$V_{xx}^{\text{mol}}(\mathbf{r}_b) = \zeta_b (2/15) (2P_{(2p_{xb}|2p_{xb})} - P_{(2p_{yb}|2p_{yb})} - P_{(2p_{zb}|2p_{zb})}) \quad (16)$$

Only the one-centre integrals are calculated. $2p_x$ is a Slater orbital and ζ is the orbital exponent.

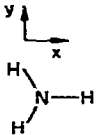
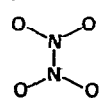
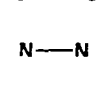
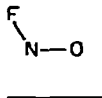
In Table 1 different calculations of the EFG for some molecules are compared. It can be seen that semi-empirical and ab initio calculations of the EFG differ by up to a factor of two. However, in all cases the sign of the EFG is equal for both methods.

The external EFG is changed by the electron core around the nucleus considered (eqn. 1). Because γ_∞ -values for the ions discussed here are in the range $-1 \geq \gamma_\infty \geq -100$, they play an important role in calculating charge distributions from QCC. Besides γ_∞ , the dipole polarizability α^D and the quadrupole polarizability α^Q influence the results of the lattice sums considerably. None of the three parameters γ_∞ , α^D , and α^Q is known from experiments. Unfortunately, the different methods available to calculate γ_∞ , α^D , and α^Q give remarkably differing results. This problem is less severe in evaluating the parameters for the cations than for the anions.

Mostly atomic wave functions are used for the calculations of γ_∞ , α^D , and α^Q ; in some cases the influence of the lattice on the ionic wave functions is taken into account. The parameters of Na^+ and Ba^{2+} (Table 2) were calculated for "ions in crystals" (ions in a Watson sphere) [15, 16]. However, for N, O, F, and B, a proper choice of γ_∞ , α^D , and α^Q is quite difficult. Feiok and Johnson [17] report an anti-shielding factor of $\gamma_\infty = 3000$ for the free ion N^{1+} . Schmidt and Weiss [16] found $\gamma_\infty(\text{N}^{5+}) = 0.10$ (free ion), and 0.17 (ion in crystal); $\gamma_\infty(\text{N}^{3-}) = -197$ (free ion), and -12.9 (crystal ion), respectively. From the latter value γ_∞ ca. -6.5 is interpolated for the neutral nitrogen atom under the following assumptions: the main part of γ_∞ is due to the perturbation of the outermost subshell; $\gamma_\infty(\text{N}^{3-}; 2p) = -13.6$. Assuming three $2p$ electrons for the neutral nitrogen, only half the value of $\gamma_\infty(\text{N}^{3-})$ is taken

TABLE 1

Electric field gradient (in atomic units) for some molecules at the site of the nitrogen as calculated from eqn. (16). The ab initio calculations are taken from Snyder and Basch [14]

		CNDO/2	CNDO/2D ^a	INDO	INDO/D ^a	Ab initio
	V_{xx}	0.58	0.78	0.63	0.86	0.53
	V_{yy}	0.58	0.78	0.63	0.86	0.53
	V_{zz}	-1.16	-1.57	-1.26	-1.71	-1.06
	V_{xx}	-0.24	-0.23	-0.10	-0.07	-0.15
	V_{yy}	-0.09	-0.06	-0.10	-0.08	-0.13
	V_{zz}	0.32	0.28	0.21	0.14	0.28
	V_{xx}	-0.62	-0.29	-0.54	-0.22	-0.88
	V_{yy}	0.31	0.15	0.27	0.11	0.44
	V_{zz}	0.31	0.15	0.27	0.11	0.44
	V_{xx}	-0.41	-0.15	-0.38	-0.11	-0.90
	V_{yy}	0.05	-0.06	0.05	-0.04	0.27
	V_{zz}	0.36	0.20	0.32	0.15	0.64

^aThe D indicates that these values are calculated from a deorthogonalized basis set C' , that is the matrix of the orbital coefficients C originally derived from CNDO/2 or INDO multiplied by $S^{-1/2}$, $C' = C \cdot S^{-1/2}$. S is the overlap matrix.

TABLE 2

Anti-shielding factors γ_{∞} , dipole polarizabilities α^D , quadrupole polarizabilities α^Q , nuclear quadrupole moments Q , and gross charges N_a , used for the calculations

Ion	Atom	γ_{∞}	α^D (Å ³)	α^Q (Å ³)	Nucleus	$Q \cdot 10^{24}$ (cm ²)	N_a from INDO calculations
NO ₂ ⁻	O		1.31 ^a	3.00 ^a			-0.562
	N	-6.17 ^a	1.84 ^a	6.23 ^a	¹⁴ N	0.0174 ^b	+0.124
NO ₃ ⁻	O		1.31	3.01 ^a			-0.585 ^b
	N	-4.82 ^a	1.44 ^a	4.86 ^a	¹⁴ N	0.0174 ^b	+0.754 ^b
BF ₄ ⁻	B	0.53 ^c	—	—	¹¹ B	0.04065 ^d	+0.763
	F		0.824 ^a	0.657 ^a			-0.441
Na ⁺		-4.75 ^e	0.16 ^e	0.067 ^a	²³ Na	0.101 ^f	(+1)
Ba ²⁺		-122.2 ^a	3.71 ^a	7.20 ^a	¹³⁷ Ba	0.28 ^g	(+2)

^aRef. 16. ^bN. Ensslin, W. Bertozzi, S. Kowalski, C. P. Sargent, W. Turchinets, C. F. Williamson, S. P. Fivozinsky, J. W. Lightbody, Jr. and S. Penner, Phys. Rev. C, 9 (1974) 1705. ^cM. H. Cohen, Proc. Roy. Soc. Ser. A, 269 (1962) 550. ^dR. K. Nesbet, Phys. Rev. A, 2 (1970) 1208. ^eRef. 15. ^fR. M. Sternheimer and X. R. F. Peierls, Phys. Rev. A, 3 (1971) 837. ^gG. zu Puttlitz, Ann. Physik (Leipzig), 11 (1963) 248. ^hCalculated with the coordinates of NaNO₃.

into account and $\gamma_{\infty}(\text{N}^0)$ ca. -6.5 is found by a somewhat problematic interpolation. This linear interpolation is not useful for free ions since the repulsion potential of the electron cloud has an important influence on the wave functions. Therefore, γ_{∞} does not vary linearly with the charge of the

ion, for instance going from N^{1-} to N^{3-} . Within the Watson sphere the repulsion potential is partly compensated by the potential of this charged sphere [16]. The linear interpolating procedure used here seems to be the best compromise we found.

α^D and α^Q given in Table 2 were also found from this simple interpolation.

RESULTS

To calculate the EFGs at the sites of the different nuclei of interest, the parameters shown in Table 2 were used. The lattice sums are based on the gross charges found from INDO calculations (last column of Table 2) and these charges were held constant during the iteration to self-consistency. In an independent calculation, the point charge distribution within the molecular ions was adjusted to fit η_{calc} to η_{exp} .

For the calculations a rigid lattice is assumed, whereas the experimental data have been determined at finite temperatures between 4.2 K and room temperature, depending on the substance considered. The ^{14}N NQR results on sodium nitrite were extrapolated down to 0 K and corrected for zero-point vibrations [18, 19]. For the other EFGs discussed here, no such corrections are available. This should be kept in mind when comparing experiment and calculation.

NaNO_2

Sodium nitrite, NaNO_2 , has been investigated experimentally and theoretically many times. In Table 3 the charge distributions in the nitrite ion as found by different authors are listed. The values for the gross charge at the nitrogen range from $-0.37e$ to $+1.14e$. Using a semi-empirical method to calculate the multipole moments of the NO_2^- group and taking these moments into account in the lattice summation, Betsuyaku [20] calculated the EFG(^{23}Na) in NaNO_2 . The results are not satisfactory.

TABLE 3

Gross charge N_N calculated for the nitrogen atom in NaNO_2 , by several authors using different methods

N_N	Method	Ref.
0 ± 0.2	^{14}N -NQR and Townes and Dailey theory	19
-0.37	^{14}N -NQR	18
$+0.20$	Double- ζ ab initio calculation of the free NO_2^- ion	21
$+0.1586$		22
-0.36	Calculation of the spontaneous polarization by a simple point charge model	23
$+1.14$	Point charge model	2
-0.27	Extended point charge model	
	$\left\{ \begin{array}{l} \eta \text{ adjusted to the} \\ \text{exp. value of the} \\ ^{23}\text{Na resonance} \end{array} \right.$	This work

From measurements of $e^2qQ/h(^{23}\text{Na})$ on single crystals at room temperature by Weiss [24], Weiss and Biedenkapp [25], and Betsuyaku [26], $e^2qQ/h(^{23}\text{Na}) = 1100$ kHz and $\eta(^{23}\text{Na}) = 0.1092$ were found. By extrapolation to 0 K and correction for zero-point motion of the ^{14}N NQR measurements, Ikeda et al. [18] and Marino and Bray [19] found $e^2qQ/h(^{14}\text{N}) = 6048$ kHz and $\eta(^{14}\text{N}) = 0.426$, and $e^2qQ/h(^{14}\text{N}) = 6135$ kHz and $\eta(^{14}\text{N}) = 0.435$, respectively.

The room temperature phase of NaNO_2 crystallizes in the orthorhombic crystal system (see Fig. 5). With the coordinate system x , y , and z chosen, the orientation of the EFG tensor at the nucleus ^{23}Na is at room temperature determined by $x \parallel V_{xx}$; $y \parallel V_{yy}$; $z \parallel V_{zz}$. Unfortunately, the direction cosines of the EFG tensor of ^{14}N in NaNO_2 have not been determined experimentally. They are assigned here to reach best agreement between the calculated and measured components of the EFG tensor. For the calculation of the EFG the atomic coordinates determined by Carpenter [27] are used which are in good agreement with neutron diffraction data of Kay and Frazer [23]. In Table 4 the results of our calculations are given.

From the lattice summation, plausible results for the EFG at the site of the ^{23}Na nucleus are found. Starting with the charge distribution of the NO_2^- ion determined by INDO calculations (which is in good agreement with the above mentioned double- ξ calculations), the z axis of the EFG tensor is in the correct crystallographic direction. However, $V_{xx}(\text{calc})$ is rotated by 90° with respect to $V_{xx}(\text{exp})$ (see line 9, Table 4) and η_{calc} is considerably larger than η_{exp} . If the asymmetry parameter $\eta(^{23}\text{Na})$ is adjusted to the experimental value, a charge of $-0.27e$ is derived for the nitrogen (see line 10, Table 4). The absolute values V_{ii} are close to the experimental ones. In Table 4, lines 1 and 4, it can be seen that simple point charge calculations of the nitrogen charge give wrong results. Only a consideration of induced

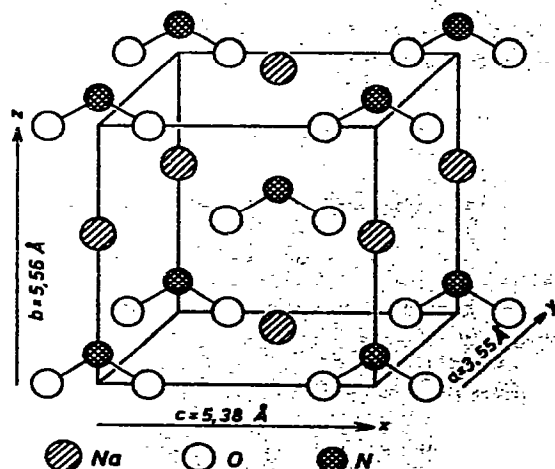


Fig. 5. Unit cell of NaNO_2 , space group $C_{2v}^{10}/Imm2$. The crystal axes a , b , and c are the main axes of the EFG at the site of the sodium. The positions of the atoms are [27]: $(0, 0, 0; 1/2, 1/2, 1/2) +$; N in $2a$: $(0, t, 0)$ $t = 0.1188$; Na in $2a$: $(0, w, 0)$ $w = 0.5862$; O in $4d$: $(0, u, v; 0, u, \bar{v})$ $v = 0.1944$ and $u = 0.0$.

TABLE 4

Components V_{ij} of the electric field gradient tensor in NaNO_2 at the site of the nuclei ^{23}Na and ^{14}N , respectively. The components V_{ij} are given in units of $e \cdot 10^{21} \text{ cm}^{-1}$. The gross charge of the nitrogen atom given in lines 1–3 and 9 is taken from the INDO calculations of the nitrite ion, those in lines 4–6 and 10 are derived by adjusting $\eta_{\text{calc}}(^{23}\text{Na})$ to $\eta_{\text{exp}}(^{23}\text{Na})$

Line	Gross charge at the nitrogen atom.	Contributions to the EFG	EFG(^{23}Na)			EFG(^{14}N)				
			V_{xx}	V_{yy}	V_{zz}	η	V_{xx}	V_{yy}	V_{zz}	η
<i>Lattice</i>										
1	0.124	Point charges P	-2.95	+2.79	+0.161	0.89	+2.19	-9.52	+7.33	0.54
2	(INDO)	P + ind. dipole moments D	-2.75	+2.31	+0.439	0.68	+2.18	-9.48	+7.30	0.55
3		P + D + ind. quadrupole moments	+2.34	+0.958	-3.29	0.42	+1.25	-8.06	+6.81	0.69
4	1.15	Point charges P	-3.96	-4.94	+8.90	0.109	+2.51	-7.94	+5.42	0.37
5	1.06	P + ind. dipole moments D	-3.32	-4.15	+7.40	0.109	+1.74	-6.94	+5.21	0.49
6	-0.270	P + D + ind. quadrupole moments	+3.09	+3.85	-6.94	0.109	+1.08	-8.52	+7.44	0.75
<i>Molecule</i>										
7		2 Intratonic O-atoms					-66.7	+59.0	+7.7	-
8		p-Electrons of N					+174.9	+484.7	-659.6	0.47
<i>Sum</i>										
9	0.124	Line 3 · (1 - γ_∞) + lines 7 + 8	+13.43	+5.51	-18.94	0.42	+115.5	+496.8	-612.3	0.62
10	-0.270	Line 6 · (1 - γ_∞) + lines 7 + 8	+17.78	+22.12	-39.90	0.109	+114.5	+494.1	-608.6	0.62
11		Experiment [24, 18]	+13.93	+17.36	+31.29	0.109	+286.6	+711.8	+998.3	0.43

dipole and quadrupole moments leads to a reasonable charge at the nitrogen (see line 10). In the reported calculations the polarizability of Na^+ was neglected. Taking the value $\alpha^{\text{D}}(\text{Na}^+) = 0.16 \text{ \AA}^3$ [15], the new values for the EFG are shifted less than 1%. Therefore, the polarizability of Na^+ has been neglected in all self-consistent calculations of this work.

It is interesting to study the influence of α^{D} and α^{Q} on the EFG at the site of ^{23}Na ; the results are shown in Table 5. The larger values of α^{D} and α^{Q} used are those calculated for the ions O^{2-} and N^{3-} , the smaller values for O^{6+} and N^{5+} . Comparison with experiment shows that interpolated values for α^{D} and α^{Q} (last line of Table 5) as used here are satisfactory in the multipole model calculations.

The EFG at the nitrogen site was found by using eqns. (15) and (16). The intramolecular part of the molecular ion gives the largest contribution to the EFG at the nitrogen site (see Table 4). Within the limits of the semi-empirical method (see Table 1), $\eta_{\text{calc}}(^{14}\text{N})$ is found in the right order of magnitude. However, the absolute value of the main components $V_{zz}(^{14}\text{N})$, $V_{xx}(^{14}\text{N})$, and $V_{yy}(^{14}\text{N})$ are smaller than the experimental values by a factor of two. This discrepancy is larger than the uncertainty of the quadrupole moment Q of the nitrogen nucleus, but is in the same order of magnitude as the discrepancies between the EFG gained by INDO and ab initio calculations.

NaBF_4

Sodium tetrafluoroborate, NaBF_4 , incorporates two sorts of nuclei, ^{23}Na and ^{11}B , which are convenient probes to investigate the EFG at the respective sites. NMR experiments and a determination of the crystal structure were done by Weiss and Zohner [28]. At room temperature they found $e^2qQ/h(^{23}\text{Na}) = 1008.4 \pm 1.2 \text{ kHz}$; $e^2qQ/h(^{11}\text{B}) = 59.9 \pm 0.6 \text{ kHz}$; $\eta(\text{Na}) = 0.095$; $\eta(\text{B}) = 0.65$. In Fig. 6 the coordinates used for the semi-empirical calculations of the BF_4^- ion are given. The multipole model (see Table 6) shows that in NaBF_4 the influence of the induced moments at the site of the ^{23}Na nucleus is much

TABLE 5

Influence of the polarizabilities on the calculated EFG at the site of ^{23}Na in NaNO_2 . The asymmetry parameter $\eta_{\text{calc}}(^{23}\text{Na})$ is adjusted to the experimental value at 0.109 in each case

Assumption		Result							
Ions (ionic charge)		Nitrogen		Oxygen		Gross charge at the nitrogen atom	EFG $(1 - \gamma_{\infty})/e \cdot 10^{22}$ (cm^{-2})		
		α^{D}	α^{Q}	α^{D}	α^{Q}		V_{xx}	V_{yy}	V_{zz}
N^{5+}	O^{6+}	0.07	0.5	0.06	0.24	+1.04	-20.00	-24.90	+44.89
N^{5+}	O^{2-}	0.07	0.5	1.71	3.94	-0.243	+6.53	+8.13	-14.67
N^{3-}	O^{6+}	3.85	13.0	0.06	0.24	+0.444	+6.01	+7.47	-13.48
N^{3-}	O^{2-}	3.85	13.0	1.71	3.94	-1.310	+59.91	+74.56	-134.47
$\text{N}^{0.12+}$	$\text{O}^{0.56-}$	1.84	6.23	1.31	3.00	-0.270	+17.78	+22.12	-39.90
Experiment [24]							+13.93	+17.36	+31.29

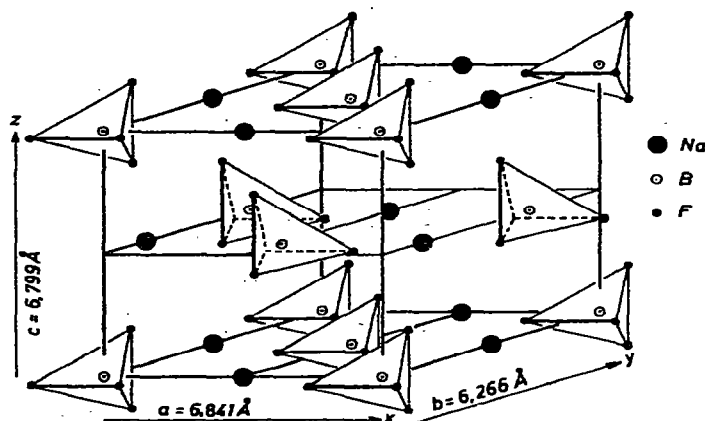


Fig. 6. Unit cell of NaBF_4 , space group $D_{2h}^{12}-Cmcm$, and the crystal axes a , b and c . x , y and z are the main axes of the EFG at the site of the sodium. The positions of the atoms are [28]: $(0, 0, 0; \frac{1}{2}, \frac{1}{2}, 0) +$; Na in $4c (0, t, \frac{1}{4}; 0, \bar{t}, \frac{3}{4})$ $t = 0.656$; B in $4c (0, u, \frac{1}{4}; 0, \bar{u}, \frac{3}{4})$ $u = 0.161$; F(I) in $8f (0, v, w; 0, \bar{v}, \bar{w}; 0, v, \frac{1}{2}-w; 0, \bar{v}, \frac{1}{2}+w)$; F (II) in $8g (x, y, \frac{1}{4}; \bar{x}, y, \frac{1}{4}; x, \bar{y}, \frac{3}{4}; \bar{x}, \bar{y}, \frac{3}{4})$ where $v = 0.290$, $w = 0.086$, $x = 0.163$, $y = 0.032$.

smaller than that found in NaNO_2 . INDO leads to a formal charge at the site of the boron which is about the same as the adjusted value (adjusting $\eta_{\text{exp}}(^{23}\text{Na})$ and η_{calc}). Good agreement between $e^2qQ/h(^{23}\text{Na})_{\text{exp}}$ and $e^2qQ/h(^{23}\text{Na})_{\text{calc}}$ is found. The influence of the polarizability on the EFG is small; a change of $\alpha^D(\text{F}^-)$ from 0.824 \AA^3 to 0.909 \AA^3 changes the adjusted charge distribution at the boron site only slightly from $0.918e$ to $0.955e$ by keeping $\eta(^{23}\text{Na})$ constant.

Unfortunately, the EFG at the boron site is not a simple physical property to judge the charge distribution in NaBF_4 ; small deformations of the fluorine tetrahedron (e.g. changes within the limits of error of the crystal structure determination) lead to changes in the calculated EFG of a magnitude comparable with the EFG found experimentally.

NaNO_3

Sodium nitrate, NaNO_3 , crystallizes with the calcite structure ($D_{3d}^6 - R\bar{3}c$, $Z = 2$). The point positions were evaluated by X-ray [29] and neutron diffraction [30]. The parameters used for the EFG calculations are given in the legend to Fig. 7. The experimental QCC is: $e^2qQ/h(^{23}\text{Na}) = 354 \text{ kHz}$, $T = 4.2 \text{ K}$ [31]; $e^2qQ/h(^{14}\text{N}) = 758 \text{ kHz}$, $T = 77 \text{ K}$ [32]. The results of our calculations are summarized in Table 7. Since η is zero at the site of ^{23}Na , the charge distribution of the nitrate group was adjusted for best agreement between $V_{zz}(\text{calc})$ and $V_{zz}(\text{exp})$ at the site of the sodium ion. There is a choice between two different charge distributions, since the sign of the EFG is not deducible from an NMR experiment. The adjusted value of $q_N = 0.832e$ (see Table 7, line 6) is in good agreement with the nitrogen charge determined by INDO calculations $q_N = 0.754e$, after which the negative sign of V_{zz} seems to be correct.

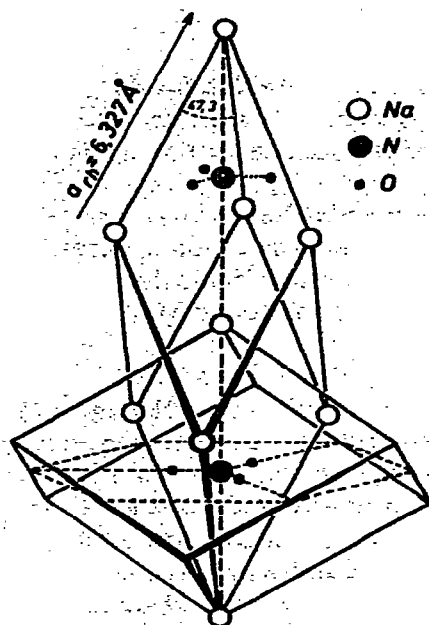


Fig. 7. Unit cell of NaNO_3 (D_{3d}^6 - $R\bar{3}c$) with rhombohedral axes. The positions of the atoms are [29]: Na in $2b$ ($0, 0, 0; \frac{1}{2}, \frac{1}{2}, \frac{1}{2}$); N in $2a$ ($\frac{1}{4}, \frac{1}{4}, \frac{1}{4}; \frac{3}{4}, \frac{3}{4}, \frac{3}{4}$); O in $6e$ ($x, \frac{1}{2}-x, \frac{1}{2}; \frac{1}{2}-x, \frac{1}{2}, x; \frac{1}{2}, x, \frac{1}{2}-x; \bar{x}, \frac{1}{2}+x, \frac{3}{4}; \frac{1}{2}+x, \frac{3}{4}, \bar{x}; \frac{1}{2}+x, \bar{x}, \frac{1}{2}+x$), where $x = 0.2448$.

TABLE 7

Electric field gradient in NaNO_3 , at the site of the ^{23}Na and the ^{14}N nucleus (V_{zz} in units of $e \cdot 10^{22} \text{ cm}^{-3}$)

Line	Gross charge at the nitrogen atom	Contributions to the EFG	EFG (^{23}Na) V_{zz}	EFG (^{14}N) V_{zz}
<i>Lattice</i>				
1	0.754 (INDO)	Point charges P	-0.244	-6.86
2		P + ind. dipole moments D	-1.288	-7.13
3		P + D + ind. quadrupole moments	-1.488	-6.531
4	0.030 1.300	Point charges P	+1.751	-5.93
5		P + ind. dipole moments D	-1.750	-7.57
6		P + D + ind. quadrupole moments	+1.751	-5.00
			-1.750	-6.65
<i>Molecule</i>				
7		3 O-atoms		+91.8
8		p-Electrons of N		+189.4
<i>Sum</i>				
9	0.754	Line 3 $\cdot (1 - \gamma_{\text{Na}})$ + lines 7 + 8	-8.558	+243.2
10	0.832	Line 6 $\cdot (1 - \gamma_{\text{Na}})$ + lines 7 + 8	-10.07	+242.4
11		Experiment [31, 32]	+10.07	+125.1

INDO calculations ($q_N = 0.769e$) and from adjusted charge distributions (see Table 8). It is seen that the EFG at the site of the barium ion depends considerably on the charge distribution of the nitrate ion (cf. lines 1 and 4 of Table 8). Owing to some self-compensation, the influence of α^D on the EFG at the barium site is found to be small. However, α^Q changes the EFG at the Ba^{2+} site considerably and the full multipole model (monopoles + dipoles + quadrupoles) leads to an approximate agreement between the INDO charges at the nitrogen and the adjusted one. The negative sign of V_{zz} at the site of the barium is derived from the calculations, as in the case of sodium nitrate for V_{zz} of sodium. The deviation between the adjusted nitrogen charge and the calculated one is slightly larger if the calculation is done with the data of Birnstock's structure determination. The experimental value at room temperature is e^2qQ/h (^{137}Ba) = 6.995 MHz and $\eta_{exp} = 0$ [36].

Since a self-consistent calculation of the EFG within the framework of the multipole model is very time consuming for $Ba(NO_3)_2^*$, the influence of the induced quadrupoles on the induced dipoles was neglected in the evaluation of the EFG (^{137}Ba) in $Ba(NO_3)_2$, in contrast to all other calculations reported here. Calculations based on the Lutz model were also done, including the influence of the quadrupoles on the dipolar field. This additional field changes the values for the nitrogen charge (line 6 of Table 8) to 0.828e and 0.159e, respectively, which is in better agreement with the results of the INDO calculations of the free ion.

The calculation of the EFG (^{14}N) in $Ba(NO_3)_2$ (see Table 9) is compared with the experimental value of e^2qQ/h (^{14}N)_{exp} = 651 kHz at room temperature, as reported by Weiden and Weiss [36]. Only one resonance is found experimentally, a result also reported by Gourdji [37]. Similarly to $NaNO_3$ at the site of the nitrogen, the lattice contribution to the EFG and the contribution of the intramolecular oxygen atoms to the EFG cancel

TABLE 8

Electric field gradient in $Ba(NO_3)_2$ at the site of the ^{137}Ba nucleus (V_{zz} in units of $e \cdot 10^{21} \text{ cm}^{-2}$)

Line	Contributions to the EFG	Gross charge at the nitrogen atom	EFG (^{137}Ba) V_{zz} coordinates [34]	Gross charge at the nitrogen atom	EFG (^{137}Ba) V_{zz} coordinates [35]
<i>Lattice</i>					
1	Point charges P	0.769(INDO)	-10.95	0.769(INDO)	-10.303
2	P + ind. dipole moments D		-10.29		-9.556
3	P + D + ind. quadrupole moments		-2.82		-1.70
4	Point charges P	0.513	-5.79	0.539	-5.79
		-0.062	5.79	-0.050	5.79
5	P + ind. dipole moments D	0.566	-5.79	0.603	-5.79
		0.041	5.79	0.091	5.79
6	P + D + ind. quadrupole moments	0.946	-5.79	0.977	-5.79
		0.257	5.79	0.387	5.79
7	Experiment/(1 - γ_{∞})		± 5.79		± 5.79
8	Experiment [36]		± 713.4		± 713.4

*For one charge distribution in the framework of the Birnstock model, a 15-min computer time on the IBM 370/168 is needed.

TABLE 9

Electric field gradient in $\text{Ba}(\text{NO}_3)_2$ at the site of the ^{14}N nucleus (V_{zz} in units of $e \cdot 10^{21} \text{ cm}^{-3}$)

Line	Contributions to the EFG	Gross charge at the nitrogen atom	EFG (^{14}N) V_{zz} coordinates [34]	Gross charge at the nitrogen atom	EFG (^{14}N) V_{zz} coordinates [35]	EFG (^{14}N) V_{zz} coordinates [35]
<i>Lattice</i>						
1	Point charges P	0.946	-144.0	0.977	-156.8	-133.3
2	P + ind. dipole moments D		-139.0		-147.9	-133.9
3	P + D + ind. quadrupole moments		-115.9		-123.9	-110.8
4	Line 3 · (1 - γ_∞)		-674.4		-721.0	-644.8
<i>Molecule</i>						
5	3 O-atoms		945		788	923
6	p-Electrons of the nitrogen		1830		2271	1873
7	Sum (lines 4 + 5 + 6)		2101		2338	2151
8	Experiment [36]		± 1074		± 1074	± 1074

one another partially and, therefore, the main contribution to the EFG is due to the *p*-electrons. The *p*-electron contribution to the EFG at the ^{14}N site is opposite in sign to the respective lattice contribution. Again, the EFG (^{14}N)_{calc} is about a factor of 2 higher than the EFG (^{14}N)_{exp}, indicating a failure of the INDO calculations in predicting good values for the intra-molecular EFG.

The results of the calculations based on the Birnstock model are given in Table 9. They show, assuming Birnstock's model to be correct, that one should observe a splitting of ca. 100 kHz of the ^{14}N NQR, arising from the different EFGs at the atoms N and N' respectively. Since the resolution of the experiments is ca. 2 kHz [36], a static deviation from the planarity of the NO_3^- ion in $\text{Ba}(\text{NO}_3)_2$ is not probable. A dynamic interruption of the planarity could not be seen in the NMR experiment of Weiden and Weiss.

ACKNOWLEDGEMENTS

We are grateful to the Fonds der Chemischen Industrie for support of this work. H. M. M. is obliged to the Studienstiftung des deutschen Volkes for a scholarship.

REFERENCES

- 1 R. Bersohn, J. Chem. Phys., 29 (1958) 326.
- 2 A. Weiss and K. Hattenbach, Z. Phys. Chem. (Frankfurt am Main), 29 (1961) 293.
- 3 S. Hafner and M. Raymond, J. Chem. Phys., 49 (1968) 3570.
- 4 B. R. A. Nijboer and F. W. DeWette, Physica (Utrecht), 23 (1957) 309.
- 5 M. P. Tosi, in F. Seitz and D. Turnbull (Eds.), Solid State Physics, Vol. 16, Academic Press, New York, 1964.
- 6 P. C. Schmidt, Master Thesis, Münster, 1969.
- 7 H. C. Bolton, W. Fawcett and I. D. C. Gurney, Proc. Phys. Soc., 80 (1962) 199.
- 8 C. K. Coogan, Aust. J. Chem., 17 (1964) 1.
- 9 J. A. Pople and D. L. Beveridge, Approximate Molecular Orbital Theory, McGraw-Hill, New York, 1970.
- 10 C. Giessner-Prettre and A. Pullman, Theor. Chim. Acta, 11 (1968) 159.
- 11 D. D. Shillady, F. P. Billingsley, II and J. E. Bloor, Theor. Chim. Acta, 21 (1971) 1.
- 12 R. S. Mulliken, J. Chem. Phys., 23 (1955) 1833.
- 13 H. M. Maurer, Master Thesis, Darmstadt, 1974.
- 14 L. C. Snyder and H. Basch, Molecular Wave Functions and Properties: Tabulated from SCF Calculations in a Gaussian Basis Set, John Wiley, New York, 1972.
- 15 E. Paschalis and A. Weiss, Theor. Chim. Acta, 13 (1969) 381.
- 16 P. C. Schmidt and A. Weiss, unpublished results.
- 17 F. D. Feiock and W. R. Johnson, Phys. Rev., 187 (1969) 39.
- 18 R. Ikeda, M. Mikani, D. Nakamura and M. Kubo, J. Magn. Resonance, 1 (1969) 211.
- 19 R. A. Marino and P. J. Bray, J. Chem. Phys., 48 (1968) 4833.
- 20 H. Betsuyaku, J. Chem. Phys., 50 (1969) 3117.
- 21 J. F. Wyatt, I. H. Hillier, V. R. Saunders, J. A. Connor and M. Barber, J. Chem. Phys., 54 (1971) 5311.
- 22 R. Bonaccorsi, C. Petrongolo, E. Scrocco and J. Tomasi, J. Chem. Phys., 48 (1968) 1497.
- 23 M. I. Kay and B. C. Frazer, Acta Crystallogr., 14 (1961) 56.

- 24 A. Weiss, *Z. Naturforsch. A*, 15 (1960) 536.
- 25 A. Weiss and D. Biedenkapp, *Z. Naturforsch. A*, 17 (1962) 754.
- 26 H. Betsuyaku, *J. Phys. Soc. Jpn.*, 27 (1969) 1485.
- 27 G. B. Carpenter, *Acta Crystallogr.*, 5 (1952) 132; 8 (1955) 852.
- 28 A. Weiss and K. Zohner, *Phys. Status Solidi*, 21 (1967) 257.
- 29 P. Cherin, W. C. Hamilton and B. Post, *Acta Crystallogr.*, 23 (1967) 455.
- 30 G. L. Paul and A. W. Pryor, *Acta Crystallogr. Sect. B*, 28 (1972) 2700.
- 31 G. J. D'Alessio and T. A. Scott, *J. Chem. Phys.*, 56 (1972) 3724.
- 32 M. Gourdji, L. Guibé and A. Peneau, *J. Phys. (Paris)*, 35 (1974) 497.
- 33 L. Vegard, *Z. Phys.*, 9 (1922) 395.
- 34 G. Lutz, *Z. Kristallogr. Kristallgeom. Kristallphys. Kristallchem.*, 114 (1960) 232.
- 35 R. Birnstock, *Z. Kristallogr. Kristallgeom. Kristallphys. Kristallchem.*, 124 (1967) 310.
- 36 N. Weiden and A. Weiss, *Proc. Congr. Ampère 18th. 2* (1974) 237.
- 37 M. Gourdji, Thesis, Centre d'Orsay, Paris, 1972.